INVESTIGATION OF A COMPOSITE TENSILE ENERGY ABSORPTION ELEMENT UNDER STATIC AND DYNAMIC LOADING

T. Bergmann[a*], S. Heimbs[a], G. Tremmel[a], M. Maier[b]

[a]*Airbus Group Innovations, 81663 Munich, Germany*
[b]*IVW, Institute of Composite Materials, Kaiserslautern University of Technology, 67663 Kaiserslautern, Germany*
**tim.bergmann@eads.net*

Keywords: Composites, energy absorption, tensile loading, bearing mode

Abstract
An experimental study was conducted to investigate the energy absorption capability of a tensile energy absorber, in which a metallic bolt is continuously pulled in in-plane direction through a composite or sandwich plate, causing it to fail successively under bearing mode. The presented study addresses the influence of various parameters such as fibre and matrix material, fibre architecture and angle as well as loading rate on the specific energy absorption. Furthermore, a modelling approach for the energy absorber with Abaqus/Explicit is presented.

1. Introduction

The field of application for energy absorbers reaches from passenger transportation such as automotive, railway and aircraft structures to occupational and recreational safety. Their main purpose is to protect vulnerable components (e.g. passengers, workers, sportsmen) from severe injuries by reducing the loads or decelerations caused by a collision or crash event to a survivable extent. This is typically achieved by a controlled deformation or destruction of the energy absorbing structure or component.

The energy absorption via crushing and fragmentation of fibre-reinforced plastic (FRP) materials is well known for its high weight-specific energy absorption (SEA), resulting in numerous absorber applications like crushable longitudinal members for sports cars or high-speed trains. In most of the cases, such energy absorbers are loaded in compression. In some cases tensile energy absorbers are required to absorb the crash energy under tensile loading, though. One example are fall arresting devices, protecting sportsmen or workers from fatal injuries falling from heights [1,2,3,4]. Combining the high SEA from crushing and fragmentation of FRP materials with the tensile load case, results in a tensile energy absorber concept pulling a metallic bolt in in-plane direction through a composite plate (Figure 1). This energy absorbing concept invented by Extra in [5] was initially investigated as an option for tensile absorbers for overhead stowage bins in aircraft cabins [6,7,8]. Furthermore, the suitability of this absorber concept for aircraft seats was studied in [9,10]. Other publications can be found with similar tensile tests characterising the bearing and residual strength of a pinned or bolted connection without the intention to use this mechanism for energy absorption by pulling the fastener for a specific distance through the composite structure [11,12,13].

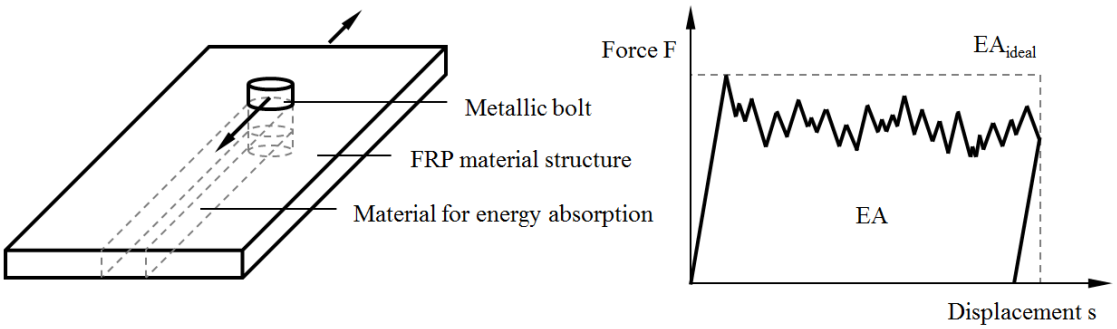

Figure 1: Schematic of a tensile energy absorber based on bolt pull-through in in-plane direction

In order to compare different energy absorber concepts, there are several specific values for quantifying the functionality and efficiency of distinct energy absorber concepts and mechanisms, respectively (Equation (1) and (2)). The SEA, defined as the absorbed energy EA, which is the area under the force-displacement-curve, divided by the absorber mass $m_{absorbed}$ used for energy absorption, is the most commonly used value. However, it is mandatory to know if the SEA values are defined on material or absorber level. Whereas on material level, no mass of supporting structure facilitating the functionality of the considered absorber is included, on absorber level the energy absorption is divided by the total absorber mass, resulting in lower SEA values depending on the specific absorber. The efficiency η is defined as the ratio between the energy absorbed EA and the energy absorbed by an ideal absorber without any losses.

$$SEA = \frac{EA}{m_{absorbed}} = \frac{1}{m_{absorbed}} \int_0^s F(s)ds \tag{1}$$

$$\eta = \frac{EA}{EA_{ideal}} = \frac{EA}{F_{\max} \cdot s_{\max}} \tag{2}$$

Because only very few data exist on the energy absorption capability of a bolt being continuously pulled through a composite or a sandwich plate, an extensive test campaign was conducted. The results are presented in this context, giving a comprehensive study on the influence of the fibre and matrix material as well as the fibre architecture and angle on the energy absorption capability of the presented tensile energy absorption concept under quasi-static and high-rate dynamic loading. Besides the experimental study, a numerical study of the energy absorption concept was conducted using a user-defined material model (VUMAT) for woven fabric composite materials in Abaqus/Explicit.

2. Specimen manufacturing

The monolithic composite material plates, mostly made of 8 plies of woven fabric material, were manufactured via vacuum assisted process (VAP). The specimens with thicknesses between 1.3 mm and 2.7 mm, depending on fibre areal weight (FAW) of the used fabric material, were cut in plates with the size of 150 mm x 75 mm via water jet cutting both in 0°/90° and ±45° direction, relative to the warp and weft directions. For the clamping of the specimen, the plates had to be drilled with 6 x M6 clearance holes according to the dimensions of the clamping device. Furthermore, the 8 mm bolt hole was chamfered from both sides in order to act as a trigger by reducing the initial peak load (Figure 2). Table 1

gives an overview of the tested composite material combinations referred to as specimen types (A) to (L).

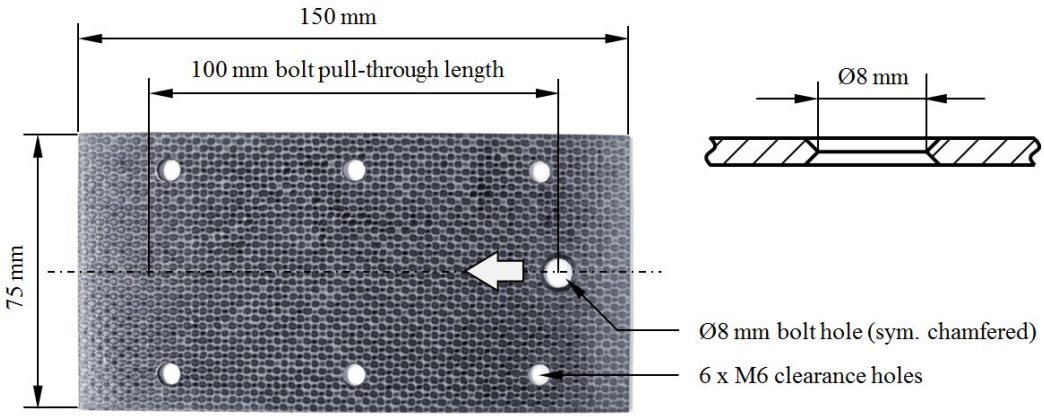

Figure 2: Dimensions of the composite specimens

Type		Fibre		Matrix
A	CF	HTA carbon fibre fabric (plain weave, 200 g/m²)	EP	Hexcel RTM6 epoxy resin
B	CF	HTA carbon fibre fabric (plain weave, 200 g/m²)	EP	Cytec EP2400 toughened epoxy resin
C	CF	HTA carbon fibre fabric (plain weave, 200 g/m²)	PEEK	Thermoplastic polyetheretherketone
D	CF	HTS carbon fibre 3D weave (2720 g/m²)	EP	Hexcel RTM6 epoxy resin
E	CF	HTS carbon fibre UD $[60°/90°/-60°/60°/90°/-60°]_s$	EP	Cytec 977-2 epoxy prepreg
F	CF	T800S carbon fibre UD $[45°/90°/-45°/0°/45°/-45°/0°/0°/90°]_s$	EP	Hexcel M21 toughened epoxy prepreg
G	GF	E-glass fibre fabric (plain weave, 390 g/m²)	EP	Hexcel RTM6 epoxy resin
H	AF	HM Aramid fibre fabric (plain weave, 170 g/m²)	EP	Hexcel RTM6 epoxy resin
I	LCP	Vectran® liquid crystal polymer fabric (twill weave 2/2, 200 g/m²)	EP	Hexcel RTM6 epoxy resin
J	UHMW -PE	Dyneema® SK65 ultra-high-molecular-weight polyethylene fibre fabric (plain weave, 130 g/m²)	EP	Epikote L20 epoxy resin
K	GF	E-glass fibre fabric (satin weave 1/4)	PA	Thermoplastic polyamid
L	GF	E-glass fibre fabric (satin weave 1/8)	PF	Phenolic resin prepreg

Table 1: Overview of fibre/matrix combinations of tested composite specimens

Sandwich specimens made of glass fibre skin and aramid honeycomb core material with different ply numbers and total thicknesses were prepared for testing, having the same dimensions as the monolithic composite specimens (Figure 2). To investigate the influence of the direction of the honeycomb core material, specimens in both core directions (L- and W-direction) were cut out of the sandwich panels. The through thickness clamping of the specimens required the core material to be partially removed and replaced by wooden ledges. In total three different sandwich materials referred to as type (M) to (O), each in L- and W-orientation, were tested under quasi-static and high-rate dynamic tensile conditions.

3. Static and high-rate dynamic absorber testing and discussion

For the planned test campaign, a special test device was developed that enables the clamping of composite and sandwich plates presented in section 2 with thicknesses between 1 mm and 20 mm. The clamping device was designed for quasi-static and high-rate dynamic testing machines and allows for maximum pulling forces of 20 kN. The plates were clamped via six bolts to ensure that no relative displacement of the plates occurred during the bolt pull-through tests. A steel bolt with a diameter of 8 mm was chosen to be pulled through the specimen making the results of this test campaign directly comparable to the studies presented in [6,7]. Figure 3 shows the test device and quasi-static bolt pull-through test setup.

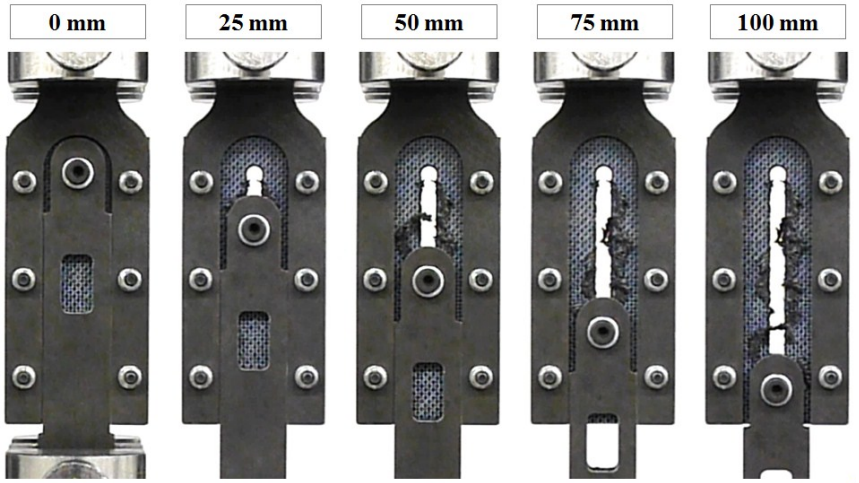

Figure 3: Image sequence of bolt pull-through test for specimen type (C) 0°/90° fibre orientation

All quasi-static tests were performed at room temperature on a Zwick universal testing machine with a loading rate of 200 mm/min. The high-rate dynamic tests with loading rates of 3 m/s were also performed at room temperature on a servo-hydraulic Zwick HTM testing machine in order to investigate the potential strain rate effects for the energy absorption element under realistic loading rates. During the tests the force-displacement-curves were measured, from which the SEA could be derived using Equation (1). For ease of comparison, the force was divided by the cross-sectional area of the bolt diameter and the plate thickness to obtain the bearing or failure stress. Three specimens were tested for every configuration resulting in a total number of about 90 tests. Figure 4 shows failure stress versus displacement curves for CF/PEEK specimens (C) as a function of the fibre orientation and loading rate.

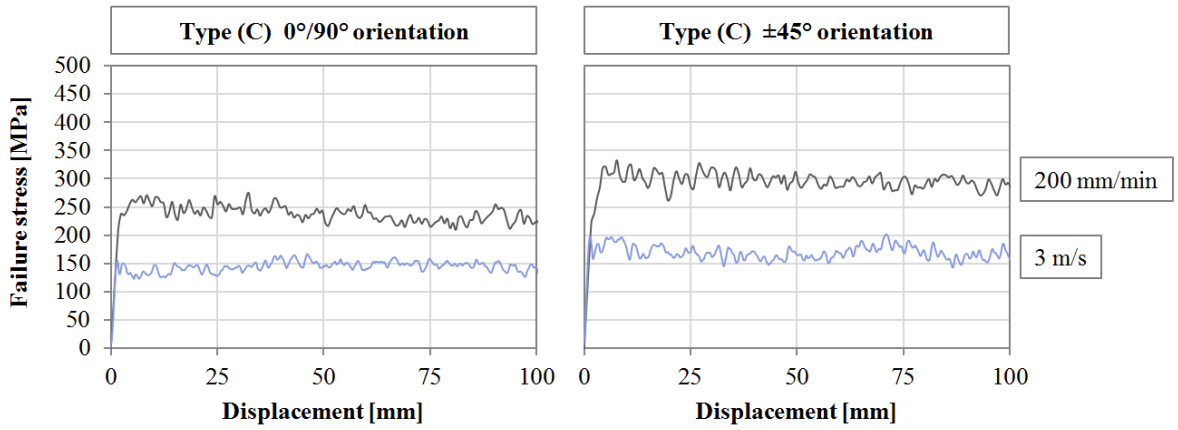

Figure 4: Failure stress vs. displacement for specimen type (C) CF/PEEK in 0°/90° (left) and ±45° (right) fibre orientation as a function of the loading rate

The micrograph of configuration type (C) 0°/90° orientation shows a debris wedge in front of the bolt that is driven through the specimen resulting in delamination failure in the plate centre and bending failure of the remaining outer plies. Depending on the fibre angle the fragments were either bent outwards remaining at the sides of the slot (0°/90° orientation) or completely separated forming a congregation of fragments driven in front of the bolt (±45° orientation). Table 2 gives an overview of failure stress, efficiency and SEA values for the tested configurations as a function of the quasi-static (QS) and dynamic loading rate.

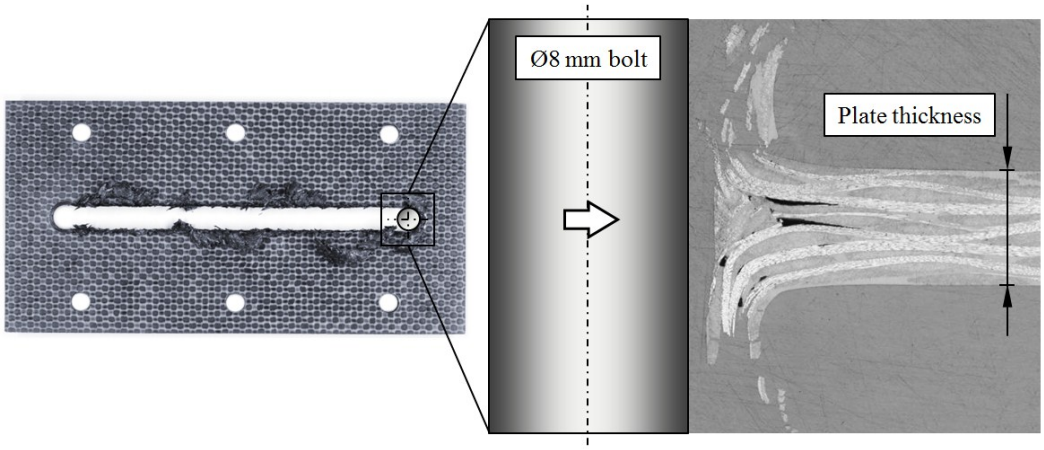

Figure 5: Micrograph of type (C) 0°/90° fibre orientation

Type	Conf.	Failure stress [MPa]		Efficiency [%]		SEA [kJ/kg]	
		QS	Dynamic	QS	Dynamic	QS	Dynamic
A	0°/90°	194,8	144,1	81,8	83,9	135,3	100,1
	±45°	238,8	155,1	85,1	86,1	164,7	107,0
B	0°/90°	238,1	145,4	86,2	83,1	158,7	96,9
	±45°	291,1	172,6	72,5	84,8	**194,1**	115,1
C	0°/90°	240,6	145,5	85,6	83,8	155,2	93,9
	±45°	281,2	173,2	83,8	82,8	181,4	111,7
D	0°/90°	383,1*	-	56,4*	-	102,2*	-
	±45°	-	-	-	-	-	-
E		309,4	-	83,3	-	173,6	-
F		315,6		82,0		180,5	
G	0°/90°	291,1	202,2	85,4	83,8	164,4	114,2
	±45°	278,0	222,3	77,2	74,9	157,1	125,6
H	0°/90°	205,7	173,2	86,7	89,3	158,3	**133,2**
	±45°	306,6*	-	49,9*	-	94,3*	-
I	0°/90°	179,1	104,7	86,8	83,6	139,9	81,8
	±45°	292,0*	-	50,3*	-	91,3*	-
J	0°/90°	170,4	105,4	80,2	88,3	160,8	99,4
	±45°	366,2*	-	48,0*	-	138,2*	-
K	0°/90°	265,3	-	90,0	-	158,8	-
	±45°	241,7	-	90,5	-	143,9	-
L	0°/90°	115,8	137,7	78,1	80,8	65,2	77,8
	±45°	156,5	144,2	69,4	81,1	85,8	81,5
M	L-dir.	29,3	28,5	82,7	81,1	81,5	79,3
	W-dir.	31,4	28,2	84,2	84,0	87,2	78,3
N	L-dir.	34,0	32,3	88,2	85,2	**94,5**	89,6
	W-dir.	32,4	32,5	82,4	85,0	89,9	**90,1**
O	L-dir.	11,9	12,6	80,8	71,2	59,6	63,1
	W-dir.	14,0	14,2	68,3	81,2	69,9	70,9

Table 2: Overview of failure stress, absorber efficiency and SEA on material level for the tested configurations

3.1. Influence of fibre material

Comparing the influence of different fibre materials with similar plain weave fabric configuration in 0°/90° orientation on the energy absorption capability led to highest SEA values for glass (G) and aramid (H), followed by Vectran® (I), Dyneema® (J) and carbon (A) fibres.

3.2. Influence of resin material

Switching from relatively brittle RTM6 epoxy resin to toughened epoxy resin EP2400 led to a strong increase of about 18 % for 0°/90° and ±45° orientation. Using a thermoplastic resin such as PEEK in combination with carbon fibres resulted in comparable SEA values as for the toughened epoxy resin. For glass fibre materials the substitution of RTM6 epoxy resin with PA6 had a negligible effect on the SEA values, whereas phenolic resin showed by far the weakest performance resulting in lowest SEA values.

3.3. Influence of unidirectional vs. 2D fabric vs. 3D fabric

Specimens with a lay-up of unidirectional plies and comparable untoughened and toughened epoxy resin materials showed 15-30 % higher SEA values than woven fabric specimens under 0°/90° orientation, although the mass $m_{absorbed}$ was increased by 10 % because of the extensive fibre pull-out at the top and bottom surface of the specimens, and no increase in SEA values for ±45° fabric orientation using carbon fibres. The use of 3D-woven fabrics led to no improvement, because no stable bolt pull-through behaviour could be achieved (values marked with *, Table 2).

3.4. Influence of fibre orientation angle

Changing the fabric orientation angle from 0°/90° to ±45° relative to the bolt direction led to an increase in SEA values of about 10-20 % for carbon fibres (A, B and C). This can be related to the highest tensile forces acting in ±45° relative to the bolt direction and therefore correlates to the fibre direction [7]. However, the stress displacement curves for the ±45° orientation are typically more oscillating and less uniform and reproducible, which can be seen by the generally lower efficiency values for the specimen with ±45° orientation. The same comparison between 0°/90° and ±45° orientation for configurations with ductile fibres (H, I and J) was not possible, because all of the configurations did not fail in a controlled and reproducible manner (values marked with *, Table 2).

3.5. Influence of loading rate

The loading rate had a significant influence on the energy absorption capability of the tested material configurations (Figure 4, Table 2). The change in loading rate from quasi-static (200 mm/min) to high-rate dynamic loading (3 m/s) resulted in a decrease in crushing stress and hence a reduction in SEA values by 20-40 %. This is in agreement with literature data of dynamic crushing of composite structures which also showed 20-40 % reduction in crushing stress levels at comparable or even higher test velocities [7,13,14,15,16].

3.6. Energy absorption capability of sandwich structures for bolt pull-through absorbers

Even though the bearing stress of the tested sandwich plates is low compared to the monolithic FRP material plates, in relation to the low specimen density the SEA values of about 60-90 kJ/kg are still competitive. The energy absorption capability was relatively unaffected by the change in loading rate from quasi-static to dynamic and the core directions.

4. Simulation

Besides the experimental test campaign, a numerical simulation study of the energy absorption mechanism was performed using the explicit nonlinear finite element code Abaqus/Explicit. The woven fabric materials were modelled via a user-defined material model (VUMAT) for woven fabric composites materials based on the Ladeveze model [17,18]. For the chosen material HTA/RTM6 (type A), a complete material characterization in warp, weft and shear direction was conducted, obtaining the material parameters needed. The model consisted of a rigid bolt and a composite plate using a layered shell approach. Using a stacked shell approach with delamination interfaces resulted in unstable model behaviour and was not further investigated. Figure 6 shows a time sequence of the simulation model and the filtered stress versus displacement curve for 0°/90° orientation.

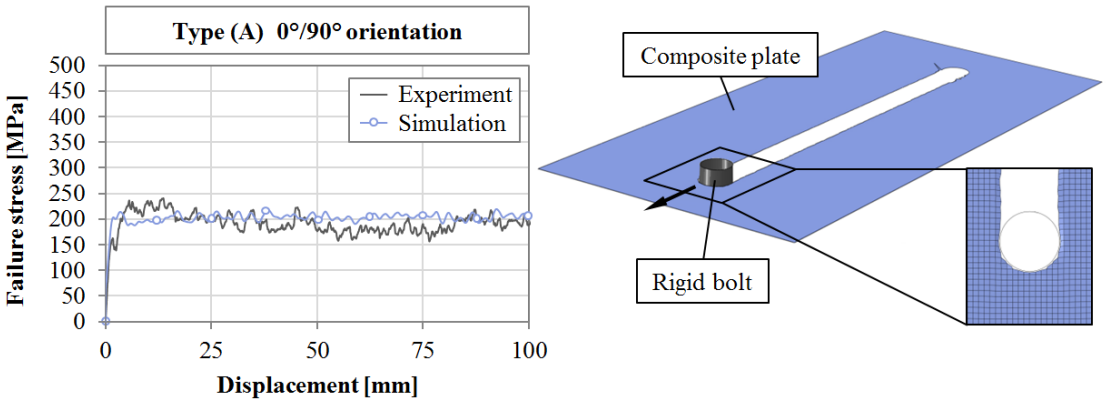

Figure 6: Simulation results (filtered) compared to experimental failure stress vs. displacement behaviour

The presented modelling approach is not capable of capturing the real crushing behaviour of the composite plates under continuous bolt pull-through loading, because of the finite discretisation of the region in front of the bolt, the missing interlaminar failure and strain rate model. Moreover, the simulation model was quite sensitive to modelling parameters like element length, frictional coefficient between bolt and composite plate as well as material parameters for the woven fabric material model such as intralaminar fracture energy G_f, all having a strong influence on the stress-displacement-behaviour. Nevertheless the influence of the fibre orientation (0°/90°, ±45°) on the quasi-static stress-displacement-curve with about 20 % higher bearing stress values for the ±45° orientation could be obtained.

5. Conclusion

Investigating the energy absorption capability of a composite tensile energy absorber element, an experimental and numerical study was conducted pulling a metallic bolt in in-plane direction through a composite structure. For the quasi-static load case SEA values of 65-195 kJ/kg were achievable, while strain rate effects during high-rate loading tests resulted in considerable reduction in SEA values of 20-40 %. The sandwich specimens did not reach the

energy absorption capability of the monolithic structures. Modelling the tensile absorber with Abaqus/Explicit, using a layered shell approach combined with a user-defined material for woven fabric composite materials, showed a good agreement to the experiments, even though the results were quite sensitive to modelling parameters.

Acknowledgement

This work was funded by BMWi in the framework of LuFo IV-4 project INCCA.

References

[1] J. P. Martin. Selection and use of fall protection and rescue equipment for work on towers. In *6th International Conference on Transmission and Distribution Construction and Live Line Maintenance (ESMO-93)*, Las Vegas, 12-17 Sept., pp. 117-126, 1993.

[2] K. Baszczynski. Influence of weather conditions on the performance of energy absorbers and guided type fall arresters on a flexible anchorage line during fall arresting. *Safety Sci.*, 42(6):519-536, 2004.

[3] A. B. Spierings and R. Stämpfli. Methodology for the development of an energy absorber. *Int. J. Impact Eng.*, 32(9):1370-1383, 2006.

[4] Y. M. Goh and P. E. D. Love. Adequacy of personal fall arrest energy absorbers in relation to heavy workers. *Safety Sci.*, 48(6):747-754, 2010.

[5] W. Extra. *Mechanische Absorptionsvorrichtung*. Pat. doc., DE 199 26 085 A1, 2000.

[6] M. Pein, D. Krause, S. Heimbs, P. Middendorf. Innovative energy-absorbing concepts for aircraft cabin interior. *International Workshop on Aircraft System Technologies (AST 2007)*, Hamburg, 2007.

[7] M. Pein. *Entwicklungsmethode für Hochleistungswerkstoffe am Beispiel von Energieabsorbern für Flugzeugkabinen*. Phd thesis, TU Hamburg-Harburg, 2009.

[8] M. Pein, D. Krause, P. Middendorf. *Mechanische Absorptionsvorrichtung*. Pat. doc., DE 10 2007 014 464 A1/B4, 2008.

[9] C. Olschinka and A. Schumacher. Dynamic simulation of flight passenger seats. In *5th LS-Dyna Forum*, Ulm, pp. 41-58, 2006.

[10] C. Olschinka and A. Schumacher. Flight passenger seats - Research on crash load cases. *Mobiles - Fachzeitschrift für Konstrukteure*, 32, pp. 62-64, 2006.

[11] M. Postec, E. Deletombe, D. Delsart, D. Coutellier. Study of the influence of the number of inter-ply interfaces on the bearing rupture of riveted composite assemblies. *Compos. Struct.*, 84(2):99-113, 2008.

[12] Y. Pekbey. The bearing strength and failure behavior of bolted E-glass/epoxy composite joints. *Mech. Compos. Mater.*, 44(4):397-414, 2008.

[13] G. S. Ger, K. Kawata, M. Itabashi. Dynamic tensile strength of composite laminate joints fastened mechanically. *Theor. Appl. Fract. Mec.*, 24(2):147-155, 1999.

[14] D. Dormegnie, D. Coutellier, D. Delsart, E. Deletombe. Studies of scale effects for crash on laminated structures. *Appl. Compos. Mater.*, 10(1):49-61, 2003.

[15] A. G. Mamalis, Y. B. Yuan, G. L. Viegelahn. Collapse of thin-wall composite sections subjected to high speed axial loading. *Int. J. Vehicle Des.*, 13(5/6):564-579, 1992.

[16] P. H. Thornton, J. J. Harwood, P. Beardmore. Fiber-reinforced plastic composites for energy absorption purposes. *Compos. Sci. Technol.*, 24(4):275-298, 1995.

[17] A.F. Johnson and J. Simon. Modelling fabric reinforced composites under impact loads. In *Euromech 400: Impact and Damage Tolerance of Composite Materials and Structures*, London, 27-29 Sept., 1999.

[18] Dassault Systèmes Simulia. *VUMAT for fabric reinforced composites*. Online doc., Answer-ID 3749, http://simulia.crusthelp.com, last access in May 2013.